

Numerical Simulation of Coherent Error Correction

Daniel Crow,* Robert Joynt, and Mark Saffman
*Department of Physics, University of Wisconsin-Madison,
1150 University Avenue, Madison, Wisconsin 53706*
(Dated: January 1, 2019)

A major goal in quantum computation is the implementation of error correction to produce a logical qubit with an error rate lower than that of the underlying physical qubits. Recent experimental progress demonstrates physical qubits can achieve error rates sufficiently low for error correction, particularly for codes with relatively high thresholds such as the surface code and color code. Motivated by experimental capabilities of neutral atom systems, we use numerical simulation to investigate whether coherent error correction can be effectively used with the 7-qubit color code. The results indicate that coherent error correction does not work at the 10-qubit level in neutral atom array quantum computers. By adding more qubits there is a possibility of making the encoding circuits fault-tolerant which could improve performance.

PACS numbers: 03.67.Hk, 32.80.-t, 32.80.Qk

I. INTRODUCTION

An important near-term goal in quantum information processing is the construction and operation of a high-quality logical qubit. This goal is currently being pursued in several physical systems [1–4]. One promising candidate system is an array of neutral atoms held in optical or magnetic traps [5, 6]. The quantum information is stored in atomic hyperfine clock states. This system has several attractive features: each natural qubit is identical, clock states exhibit long coherence times measured in seconds, state preparation and state measurement can be performed on msec timescales using well developed techniques of optical pumping and detection of resonance fluorescence [7, 8]. A universal set of quantum gate operations can be based on microwave and laser light for single qubit rotations together with Rydberg state mediated interactions for two-qubit, and multi-qubit, entangling gates [6].

Arrays of individually addressable qubits of this kind have been demonstrated in 1D [9, 10], 2D [11–14], and 3D [15]. Qubit numbers of order 100 have been demonstrated in 2D and 3D and in principle these numbers could be extended to several thousands using available technology. The current experimental status motivates a careful analysis of possible architectures for transitioning from demonstration experiments on small numbers of qubits to the creation of fault tolerant logical qubits suitable for scalable quantum computation.

A key decision parameter when choosing an architecture for a logical qubit is the available physical gate fidelity. Single qubit gates have already been demonstrated in a large 2D neutral atom array with fidelities between 0.99 and 0.999 [11]. While still marginal for a scalable system we anticipate that experimental progress based on composite pulse techniques and long coherence

optical lattices [16] will be able to extend the single qubit gate fidelities to the 0.9999 range and better, as has been demonstrated in several trapped ion experiments [17, 18]. The two-qubit Rydberg gate can in principle reach fidelities above 0.999 with square pulses [19, 20], and we anticipate even higher fidelities with more complex shaped pulse techniques.

The experimental status on two-qubit entanglement with Rydberg interactions is still far behind the theoretical limits, with the best reported Bell state fidelities currently $\sim 70-80\%$, [21, 22]. This is also an area of active research that plausibly will lead to significant future improvements in fidelity. An important feature of the Rydberg interaction in the context of logical qubit design is the long range nature of the interaction. This will enable beyond nearest neighbor interactions in a qubit array, and efficient implementation of multi-qubit entangling gates [23].

These technical capabilities of neutral-atom qubits motivate the search for an error-correction scheme that is optimized for the current state of this particular platform. The limitations on gate fidelity suggest the use of topological codes such as surface and color codes [24, 25], for which the fidelity requirements are somewhat less stringent than for other types of codes. However, error correction with the surface code relies on performing frequent syndrome measurements [26]. This turns out not to be well suited for neutral atom implementations for two reasons. First, the time needed for state measurements is currently several orders of magnitude longer than for gate operations. This time could be shortened with more efficient light collection designs, but will probably always be longer than gate times. Second, it is difficult to measure a single atomic qubit in an array without scattered light corrupting the state of a nearby qubit. While a number of possible solutions to this problem are under study [27], site resolved state measurements with minimal crosstalk have not yet been demonstrated in a neutral atom qubit array.

These challenges motivate the consideration of coher-

* decrow@wisc.edu

ent error correction methods [28–30] using a color code. The qubit geometry of the color code meshes well with current 2D arrays of neutral atom qubits. Furthermore, coherent error correction does not rely on state measurements. Of course, with coherent error correction entropy still has to be removed but this can be accomplished by preparation of fiducial states of ancilla qubits. This process also requires light scattering in an optical pumping process. However, the number of scattered photons needed for optical pumping is 1-2 orders of magnitude less than for state measurement which simplifies the task of site selective entropy removal in an array.

The physical requirements for achievement of coherent error correction using the color code have not been previously investigated, and it is not even known whether such a scheme can be made to work with reasonable error rates. In this paper we aim to decide whether coherent error correction using a color code can be a practical way to construct a logical qubit using a neutral atom array. For this purpose we simulate the operation of such a logical qubit using a minimal number of physical qubits.

The paper is organized as follows. In section II we will provide a brief introduction to color codes and the implementation of coherent error correction on the 7-qubit code. Section III discusses the details of our simulation, with the results of the simulation presented in section IV. Lastly, in section V we discuss the implications of the results and how they relate to the threshold theorem.

II. 7-QUBIT COHERENT ERROR CORRECTION

A. Color Codes

The 4.8.8 triangular color code family is capable of transversal implementation of the full Clifford group. Achieving a universal gate set would require additional techniques, such as magic state injection [31], but we do not address these additional issues in this paper. A distance d code requires $n = \frac{1}{2}(d^2 + 2d - 1)$ data qubits to form a single logical qubit. The 4.8.8 color code has been shown to have an error threshold of 0.082% [32]. For a more thorough description of the color code, see [24].

The simplest non-trivial case of a triangular color code is the $[[7, 1, 3]]$ code. It is useful to visualize the qubits arranged into three plaquettes of four qubits each, shown in Fig. 1. Associated with each plaquette are two *plaquette operators*

$$B_p^X = \otimes_i X_i \text{ and } B_p^Z = \otimes_i Z_i$$

where the index i ranges over all qubits in the p^{th} plaquette. These plaquette operators form the stabilizers of the color code. This stabilizer structure is equivalent to that of the 7-qubit Steane code [33].

The X and Z plaquette operators are sensitive to Z and X errors on the physical qubits, respectively. The

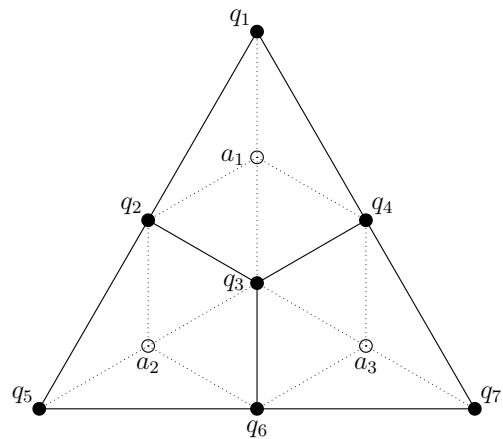


FIG. 1. Visualization of the 7-qubit color code with ancillas. The data qubits are labelled q_i and the ancillas are labelled a_i .

methods for correcting errors of different types are identical, up to a swap of X and Z operators. Therefore, for our discussion of the error correcting procedure, we will restrict ourselves to X errors detected by the B_p^Z stabilizers.

B. Coherent Error Correction

Many conventional error correction procedures rely on measurement-based error correction [1–4], in which an error syndrome is encoded on a set of ancilla qubits which are then measured. Errors are corrected based on the measured syndrome. Coherent error correction also encodes an error syndrome onto a set of ancilla qubits; however, the errors are corrected by applying unitary gates. Resetting the ancilla qubits to the $|0\rangle$ state removes the entropy from the system.

Performing coherent error correction on the 7-qubit code requires a minimum of three ancillary qubits for a total of 10 physical qubits. All together these make up one logical qubit. Each ancilla is associated with a single plaquette, and the syndrome is encoded with the circuit shown in Fig. 2. Note that this encoding circuit is not fault-tolerant, but minimizes the number of ancillary qubits required. Several distinct encoding circuits were considered, and the selected circuit was selected because it had the fewest total error insertions. The circuit in Fig. 3 demonstrates the complete error correction scheme for X -type errors. Analogous circuits are performed for Z errors. Together, the circuit will correct any single-qubit error. The sequence makes use of 3- and 4-qubit entangling gates which can be implemented using Rydberg interactions [23]. This particular circuit is well-suited to neutral-atom quantum computation but may not be practical for other physical implementations.

The circuits used for this paper could potentially be

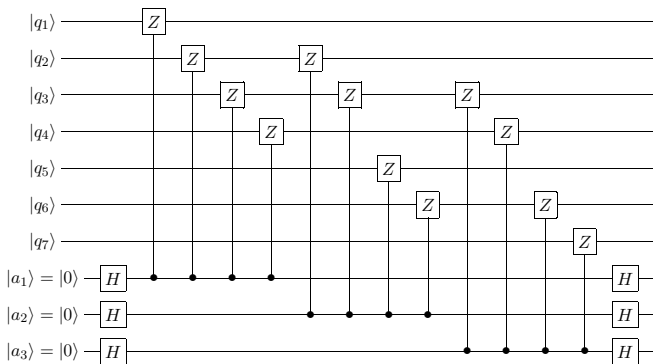


FIG. 2. Circuit to encode the syndrome detecting X . The qubits follow the same labelling scheme as in Fig. 1. The circuit elements are Hadamard gates and controlled- Z gates.

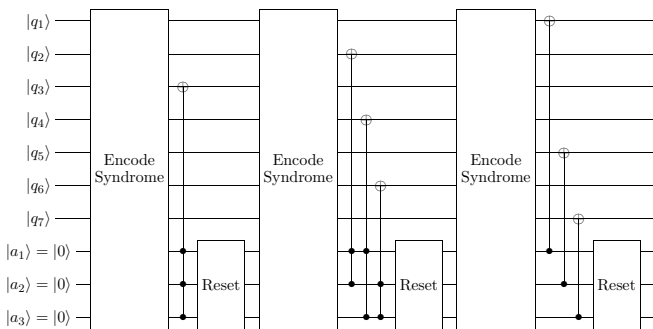


FIG. 3. The complete error correction circuit for the seven data qubits q_1 to q_7 and the three ancilla qubits a_1 , a_2 , and a_3 . The “Encode Syndrome” boxes correspond to the circuit shown in Fig. 2. The “Reset” boxes change the ancillas to the $|0\rangle$ state.

improved by making the encoding and correction circuits fault-tolerant, although this would require more physical qubits. Furthermore, this procedure could be extended to larger versions of the color code, although this presents additional obstacles. Notably, the distance d color code requires $O(d^2)$ qubits to encode the error syndrome. Thus, accessing the full error syndrome without measurement would naïvely require multi-qubit gates targeting $O(d^2)$ qubits. Due to the topological nature of the color code, simultaneous access to all syndrome values is probably not necessary, but the optimal procedure for larger color codes would require further research.

III. SIMULATION OF COHERENT ERROR CORRECTION

We performed a numerical simulation of coherent error correction using the circuits shown in the previous section. In the case of coherent error correction, the circuits performing error correction rely heavily on the ancilla qubits. In a neutral atom implementation the ancilla would be physically identical to the data qubits, so the

ancilla qubits are subject to the same error model as the data qubits in our simulation. However, the error rates of the ancilla qubits and the data qubits can be separately adjusted.

The simulation method used the full 10-qubit state vector. Each simulation began by initializing the system to the logical $|0\rangle$ state. Following initialization, each data qubit was subject to depolarizing noise characterized by the likelihood p_d of error, meant to represent accumulated error during logical operations or during hold operations as in a quantum memory.

The error-correcting circuits were then applied, characterized by the likelihood p_p of each qubit experiencing an error during a single gate (including identity gates). Thus, the errors targeted every qubit during every step, including ancillas. All noise was assumed to be depolarizing so that during each timestep the probability of any given qubit experiencing an error was p_p , and the errors were randomly and uniformly selected from the Pauli operators $\{X, Y, Z\}$. In the case of multi-qubit gates, the errors on individual qubits were uncorrelated. The simulation did not model errors due to qubit loss or measurement crosstalk. Ancilla preparation and resets were assumed to be perfect.

The calculation used state vectors instead of density matrices. This meant that the ancilla reset operations were performed by collapsing the state vector with the appropriate probabilities. Each simulation was performed many times (~ 10 million) to ensure statistical accuracy. Following error correction, we performed a measurement of the logical state and recorded the result. A measurement that returned the $|1\rangle$ logical state was counted as a failure. Comparing the number of failed simulations to the total number of simulations yields a value for the probability of logical failure, p_ℓ . Thus p_ℓ , the logical error rate in our simulation, and $1 - p_\ell$ is the chance of retaining the initial $|0\rangle$ state.

IV. RESULTS

The log-log plot in Fig. 4 shows a graph of p_ℓ vs. p_d with p_p fixed. For large p_d , the method produced values of p_ℓ better than p_d , indicating the the circuit was indeed removing error. However, for all values of p_d , the logical error rate was *worse* than the physical error rate p_p . As $p_d \rightarrow 0$, the value of p_ℓ saturates, approaching a value that was greater than p_p by an order of magnitude. This was true for all values of p_p that we investigated, varying p_p by 3 orders of magnitude. In fact $p_p = 10^{-5}$ is already a very optimistic physical error rate, so the limiting behavior raises the question of whether or not the asymptotic value of p_ℓ can ever be lower than p_p in any actual physical experiment.

The limiting value of p_ℓ can be found by setting $p_d = 0$ and comparing the logical error rate to the physical error rate. These results are shown in Fig. 5. Even testing physical error rates as low as 10^{-7} , the logical

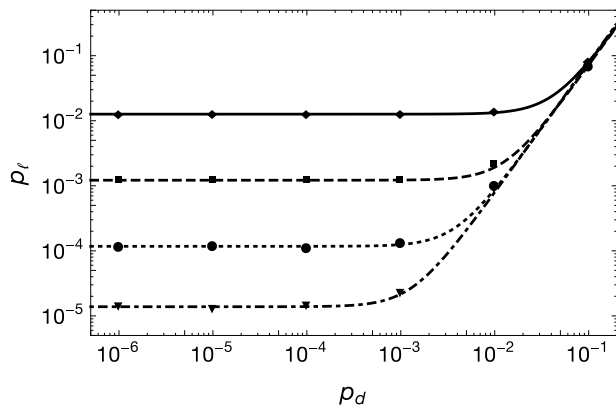


FIG. 4. Log-log plot of the logical error rate p_ℓ vs. the error rate for the data qubits p_d for various physical error rates p_p . $p_p = 10^{-3}$ (solid line), $p_p = 10^{-4}$ (dashed), $p_p = 10^{-5}$ (dotted), and $p_p = 10^{-6}$ (dot-dashed). Note all curves approach a constant as $p_d \rightarrow 0$. The curves shown are guides to the eye.

error rate p_ℓ remains larger than p_p by roughly an order of magnitude. Furthermore, the best fit line on the log-log plot gives a slope of 1.06 which indicates that the logical error rate scales linearly with the physical error rate. Assuming a proportional relation gives the best-fit result $p_\ell \approx 10.5p_p$. The simulation results show that coherent error correction is not capable of achieving a logical error rate better than the physical error rate.

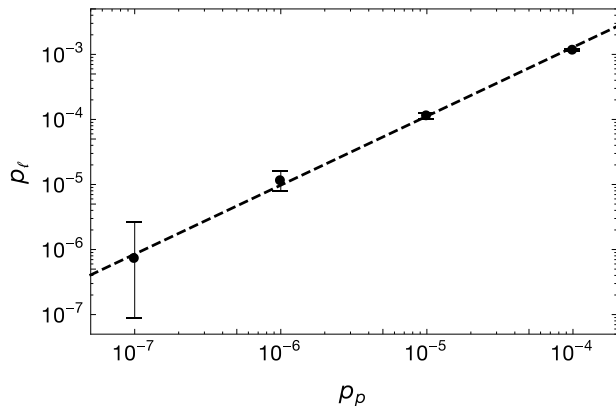


FIG. 5. Log-log plot of p_ℓ vs. p_p for $p_d = 0$ to determine the limiting behavior of p_ℓ . The dashed line shown is the best-fit line which has a slope of approximately 1.06.

In order to examine the differences between data qubits and ancilla qubits, we also calculated logical error rates as a function of the physical error rate p_a on ancilla qubits, with the physical error rate on the data qubits held constant. The results are shown in Fig. 6, showing that the logical error rate is essentially determined by the physical error rate p_p on the data qubits. Only when the p_a was several orders of magnitude greater than p_p did ancilla errors create significant changes in p_ℓ .

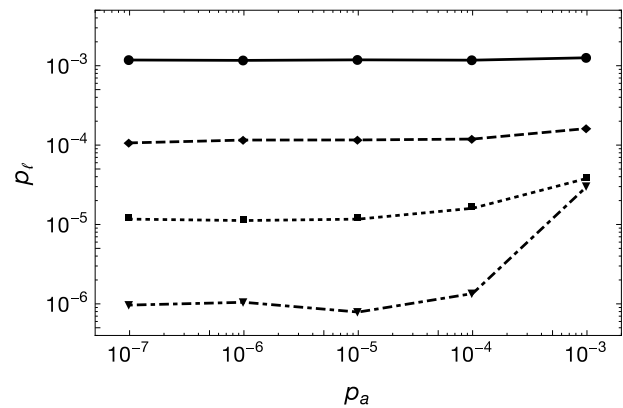


FIG. 6. Log-log plot of p_ℓ vs. p_a with $p_d = 0$. The corresponding p_p values are 10^{-4} (solid), 10^{-5} (dashed), 10^{-6} (dotted), and 10^{-7} (dot-dashed).

V. CONCLUSION

The simulations indicate that coherent error correction will not work at the level of 10 physical qubits. Furthermore, the method is difficult to implement on larger codes since gate sequences to implement coherent error correction would be significantly longer. The data strongly indicate that the coherent error correction protocol discussed in this paper produces logical error greater than physical error rate by a constant factor of ≈ 10 , suggesting that there is no threshold error rate. This difficulty does not arise because of error on the ancillas, but comes from the fact that the number of non-fault-tolerant operations involved is simply too large.

A well-known result by Aharonov and Ben-Or guarantees the existence of a threshold for certain fault-tolerant circuits [34]. However, our result does not contradict this theorem, as the theorem only guarantees the existence of a threshold for an appropriate *simulating* circuit. That is, there must exist a threshold for some fault-tolerant circuit that appropriately simulates our circuit. It should be noted that the threshold theorem holds *without* measurement. Thus, there must exist fault-tolerant coherent error correction techniques. Though implementation of such techniques is probably beyond the capabilities of current neutral atom qubit systems, the threshold result raises the question of whether or not coherent error correction on the 7-qubit code would work if the encoding circuits were made fault-tolerant.

VI. ACKNOWLEDGEMENTS

The simulations were performed using the University of Wisconsin Center for High Throughput Computing. We gratefully acknowledge the assistance of the staff. Mark Saffman acknowledges support from the IARPA MQCO program through ARO contract W911NF-10-1-0347.

-
- [1] P. Schindler, J. T. Barreiro, T. Monz, V. Nebendahl, D. Nigg, M. Chwalla, M. Hennrich, and R. Blatt, *Science* **332**, 1059 (2011).
- [2] G. Waldherr, Y. Wang, S. Zaiser, M. Jamali, T. Schulte-Herbruggen, H. Abe, T. Ohshima, J. Isoya, J. F. Du, P. Neumann, and J. Wrachtrup, *Nature* **506**, 204 (2014).
- [3] J. Kelly, R. Barends, A. G. Fowler, A. Megrant, E. Jeffrey, T. C. White, D. Sank, J. Y. Mutus, B. Campbell, Y. Chen, Z. Chen, B. Chiaro, A. Dunsworth, I. C. Hoi, C. Neill, P. J. J. O'Malley, C. Quintana, P. Roushan, A. Vainsencher, J. Wenner, A. N. Cleland, and J. M. Martinis, *Nature* **519**, 66 (2015).
- [4] D. Riste, S. Poletto, M. Z. Huang, A. Bruno, V. Vesterinen, O. P. Saira, and L. DiCarlo, *Nat Commun* **6** (2015).
- [5] T. D. Ladd, F. Jelezko, R. Laflamme, Y. Nakamura, C. Monroe, and J. L. O'Brien, *Nature* **464**, 45 (2010).
- [6] M. Saffman, T. G. Walker, and K. Mølmer, *Rev. Mod. Phys.* **82**, 2313 (2010).
- [7] A. Fuhrmanek, R. Bourgain, Y. R. P. Sortais, and A. Browaeys, *Phys. Rev. Lett.* **106**, 133003 (2011).
- [8] M. J. Gibbons, C. D. Hamley, C.-Y. Shih, and M. S. Chapman, *Phys. Rev. Lett.* **106**, 133002 (2011).
- [9] D. Schrader, I. Dotsenko, M. Khudaverdyan, Y. Miroshnychenko, A. Rauschenbeutel, and D. Meschede, *Phys. Rev. Lett.* **93**, 150501 (2004).
- [10] C. Knoernschild, X. L. Zhang, L. Isenhower, A. T. Gill, F. P. Lu, M. Saffman, and J. Kim, *Appl. Phys. Lett.* **97**, 134101 (2010).
- [11] T. Xia, M. Lichtman, K. Maller, A. W. Carr, M. J. Piotrowicz, L. Isenhower, and M. Saffman, *Phys. Rev. Lett.* **114**, 100503 (2015).
- [12] H. Labuhn, S. Ravets, D. Barredo, L. Béguin, F. Nogrette, T. Lahaye, and A. Browaeys, *Phys. Rev. A* **90**, 023415 (2014).
- [13] C. Weitenberg, S. Kuhr, K. Mølmer, and J. F. Sherson, *Phys. Rev. A* **84**, 032322 (2011).
- [14] M. Schlosser, S. Tichelmann, J. Kruse, and G. Birkel, *Quantum Information Processing* **10**, 907 (2011).
- [15] Y. Wang, X. Zhang, T. A. Corcovilos, A. Kumar, and D. S. Weiss, *Phys. Rev. Lett.* **115**, 043003 (2015).
- [16] A. W. Carr, *Improving quantum computation with neutral cesium*, Ph.D. thesis, University of Wisconsin-Madison (2014).
- [17] T. P. Harty, D. T. C. Allcock, C. J. Ballance, L. Guidoni, H. A. Janacek, N. M. Linke, D. N. Stacey, and D. M. Lucas, *Phys. Rev. Lett.* **113**, 220501 (2014).
- [18] E. Mount, D. Gaultney, G. Vrijsen, M. Adams, S. Baek, K. Hudek, L. Isabella, S. Crain, A. van Rynbach, P. Maunz, and J. Kim, "Scalable digital hardware for a trapped ion quantum computer," (2015), arXiv:1504.00035.
- [19] X. L. Zhang, A. T. Gill, L. Isenhower, T. G. Walker, and M. Saffman, *Phys. Rev. A* **85**, 042310 (2012).
- [20] T. Xia, X. L. Zhang, and M. Saffman, *Phys. Rev. A* **88**, 062337 (2013).
- [21] K. M. Maller, M. T. Lichtman, T. Xia, Y. Sun, M. J. Piotrowicz, A. W. Carr, L. Isenhower, and M. Saffman, *Phys. Rev. A* **92**, 022336 (2015).
- [22] Y.-Y. Jau, A. M. Hankin, T. Keating, I. H. Deutsch, and G. W. Biedermann, "Entangling atomic spins with a strong rydberg-dressed interaction," (2015), arXiv:1501.03862.
- [23] L. Isenhower, M. Saffman, and K. Mølmer, *Quantum Information Processing* **10**, 755 (2011).
- [24] H. Bombin and M. A. Martin-Delgado, *Phys. Rev. Lett.* **97**, 180501 (2006).
- [25] D. Nigg, M. Müller, E. A. Martinez, P. Schindler, M. Hennrich, T. Monz, M. A. Martin-Delgado, and R. Blatt, *Science* **345**, 302 (2014).
- [26] A. G. Fowler, M. Mariantoni, J. M. Martinis, and A. N. Cleland, *Phys. Rev. A* **86**, 032324 (2012).
- [27] I. Beterov and M. Saffman, "Rydberg blockade, Förster resonances, and quantum state measurements with different atomic species," (2015), arXiv:1508.07111, to appear in *Phys. Rev. A*.
- [28] V. Nebendahl, H. Häffner, and C. F. Roos, *Phys. Rev. A* **79**, 012312 (2009).
- [29] C.-K. Li, M. Nakahara, Y.-T. Poon, N.-S. Sze, and H. Tomita, *Quantum Info. Comput.* **12**, 149 (2012).
- [30] V. Nebendahl, *Phys. Rev. A* **91**, 022332 (2015).
- [31] S. Bravyi and A. Kitaev, *Phys. Rev. A* **71**, 022316 (2005).
- [32] A. J. Landahl, J. T. Anderson, and P. R. Rice, "Fault-tolerant quantum computing with color codes," (2011), arXiv:1108.5738.
- [33] A. Steane, *Proc. R. Soc. A* **452**, pp. 2551 (1996).
- [34] D. Aharonov and M. Ben-Or, *SIAM Journal on Computing*, *SIAM Journal on Computing* **38**, 1207 (2008).